Machine learning for characterizing tropical tuna aggregations under Drifting Fish Aggregating Devices (DFADs) from commercial echosounder buoys data

Y. Baidai, Laurent Dagorn, M. J. Amande, D. Gaertner, M. Capello

Machine learning for characterizing tropical tuna aggregations under Drifting Fish Aggregating Devices (DFADs) from commercial echosounder buoys data

Y. Baidai[12], L. Dagorn[1], M.J. Amande[2], D. Gaertner[1] and M. Capello[1]

[1] MARBEC, Univ Montpellier, CNRS, Ifremer, IRD, Sète, France yannick.baidai@ird.fr (corresponding author)

[2] Centre de Recherches Océanologiques (CRO), Abidjan, Côte d'Ivoire

Summary

The use of echosounder buoys deployed in conjunction with Drifting Fish Aggregating Devices (DFADs) has progressively increased in the tropical tuna purse seine fishery since 2010 as a means of improving fishing efficiency. Given the broad distribution of DFADs, the acoustic data provided by echosounder buoys can provide an alternative to the conventional CPUE index for deriving trends on tropical tuna stocks. This study aims to derive reliable indices of presence of tunas (and abundance) using echosounder buoy data. A novel methodology is presented which utilizes random forest classification to translate the acoustic backscatter from the buoys into metrics of tuna presence and abundance. Training datasets were constructed by cross-referencing acoustic data with logbook and observer data which reported activities on DFADs (tuna catches, new deployments and visits of DFADs) in the Atlantic and Indian Oceans from 2013 to 2018. The analysis showed accuracies of 75 and 85 % for the recognition of the presence/absence of tuna aggregations under DFADs in the Atlantic and Indian Oceans, respectively. The acoustic data recorded at ocean-specific depths (6 – 45 m in the Atlantic and 30 – 150 m in the Indian Ocean) and periods (4 am – 4 pm) were identified by the algorithm as the most important explanatory variables for detecting the presence of tuna. The classification of size categories of tuna aggregations showed a global accuracy of nearly 50% for both oceans.

This study constitutes a milestone towards the use of echosounder buoys data for scientific purposes, including the development of promising fisheries-independent indices of abundance for tropical tunas.

Keywords: Tropical tunas; Direct abundance indicator; Echosounder buoys; Fish Aggregating Devices; Purse seiner

1. Introduction

Many marine species are known to naturally aggregate under floating objects. Although still poorly understood, this behaviour is widely exploited by fishermen, who deploy man-made floating objects (hereafter referred to as Fish Aggregating Devices or FADs) worldwide to improve their catches (Kakuma, 2001; Fonteneau et al., 2013; Albert et al., 2014). The use of drifting FADs (DFADs) in tropical tuna fisheries was first introduced in the late 1980s in the Eastern Pacific Ocean by the US purse seine fleet (Lennert-Cody and Hall, 2001) and was later extended to all oceans and fleets from the 1990s. The instrumentation of DFADs with GPS beacons and echosounder buoys, in the mid and late 2000s respectively (Lopez et al., 2014), led to major changes in fishing strategies and behaviour of purse-seine fleets (Torres-Irineo et al., 2014). By providing skippers with almost real-time remote information on the precise location of DFADs, and on the potential presence and size of the tuna aggregation, echosounder buoys reduced the search time between two successful DFAD sets (Lopez et al., 2014). As a result, modern DFADs have significantly increase fishing efficiency (Fonteneau et al., 2013). Consequently, their use has increased considerably in the past few decades. Recent studies indicate that in less than a decade, the number of DFADs deployed in the Atlantic and Indian Oceans have increased at least fourfold (Fonteneau et al., 2015; Maufroy et al., 2017). It is estimated that over half of the annual tropical tuna purse seine catch originate from fishing sets on DFADs (Dagorn et al., 2013; Fonteneau et al., 2013).

Aside from being highly efficient fishing tools, the large number and vast spatial distribution of DFADs, coupled with their constantly evolving technology (Lopez et al., 2014), mean that they can also potentially provide unprecedented scientific insights into pelagic communities (Moreno et al., 2016; Brehmer et al., 2018). The echosounder buoys attached to DFADs regularly produce and transmit biomass estimation data. This dataset potentially holds a major opportunity for improving the management of tropical tuna stocks through the development of

fishery-independent abundance indices (Capello et al., 2016; Santiago et al., 2016). Currently, the main abundance indicators used in stock assessment for tropical tunas are derived through the standardization of Catch per Unit of Effort (CPUE) from commercial data (Fonteneau et al., 1998; Maunder et al., 2006). However, owing to the constant technological advances occurring in the purse seine fishery, it is extremely difficult to accurately standardize the CPUE time-series (Fonteneau et al., 1999). Traditionally, search time was used to quantify normal fishing effort in this fishery, however, owing to its non-random nature, the DFAD-based fishery has made this metric inconsistent over time, thus introducing major biases and uncertainties in the relationship between tuna catches and abundance (Fonteneau et al., 1999; Gaertner et al., 2015).

The need for the consideration of non-traditional data sources to provide alternate abundance indices for stock assessment of tunas is becoming increasingly apparent. In this regard, the large amount of acoustic data autonomously collected by commercial echosounder buoys on DFADs is of undeniable value. However, the direct exploitation of these data remains challenging. The biomass estimate that a buoy produces is limited by the reliability and variability of the information provided, which depends on the hardware and software characteristics of the buoy, and varies between manufacturers (Lopez et al., 2014; Santiago et al., 2016). As a result, the data provided by echosounder buoys are heterogeneous in types and formats, with limited studies having provided an assessment of their accuracy for use in scientific investigations. (Lopez et al., 2016; Baidai et al., 2017; Orue et al., 2019a).

In recent years, fisheries scientists have shown a growing interest in machine learning methods for the processing of both passive acoustic data (Roch et al., 2008; Zaugg et al., 2010; Noda et al., 2016; Malfante et al., 2018) and acoustic data collected by scientific echosounders (Fernandes, 2009; Robotham et al., 2010; Bosch et al., 2013). Despite this trend, very few studies have been conducted on the implementation of automated classification methods for analysing the extensive datasets collected by commercial vessels (Uranga et al., 2017).

This paper presents a new methodology, based on machine learning, for processing the echosounder data collected from one of the main models of echosounder buoy used to equip DFADs worldwide (Moreno et al., 2019).

2. Material and Methods

2.1. Database description

2.1.1. Echosounder buoy data

We used data from the Marine Instruments M3I buoy (https://www.marineinstruments.es), collected on DFADs deployed by the French purse seine vessels operating in the Western Indian and Eastern Atlantic oceans from 2013 to 2018. The dataset consists of more than 60 million data points collected by approximately 35 000 M3I buoys. This model of buoy includes a solar powered echosounder operating at a frequency of 50 kHz, with a power output of 500 W, a beam angle of 36°, and a sampling frequency of 5 minutes (Fig. 1A). The acoustic data are processed by an internal module that automatically converts the acoustic energy into (i) a total biomass index and (ii) 50 integer acoustic scores (ranging from 0 to 7) indicating the acoustic energy recorded within 3 m depth layers, over a total detection range of 150 meters (Fig. 1B). In the default-operating mode, the internal module stores the 50 acoustic scores that correspond to the highest total biomass index recorded every 2 hours. From here on these 50 acoustic scores will be referred to as an "acoustic sample". The assessment of the accuracy of the total biomass index calculated directly by the buoy's internal module is presented in the Supplementary Appendix A1. The set of acoustic scores which constitute the acoustic sample is transmitted via satellite to the purse seine vessel every 12 hours under default settings. During the satellite communication, the GPS position of the buoy is also recorded and transmitted.

2.1.2 Activity data on DFADs

To ground truth the echosounder buoy dataset, catch and fishing activities were obtained from fishing logbooks of purse seine vessels and on-board observer reports from 2013 to 2018 in the western Indian and eastern Atlantic oceans. Observer data were collected under the EU Data Collection Framework (DCF) and the French OCUP program (Observateur Commun Unique et Permanent), which reached a coverage rate of 100% in the Atlantic Ocean in 2015 (Goujon et al., 2018), and over 80% since 2016, in the Indian Ocean (Goujon et al., 2017). From this combined dataset, the date, time, GPS location and buoy identification code associated with (i) fishing sets, (ii) newly deployed DFADs and (iii) visits to DFADs equipped with buoys owned by the vessel and which did not result in a fishing operation, were selected to be cross-referenced with echosounder buoy dataset. For successful fishing sets on DFADs, catch data for the three primary target species; yellowfin (*Thunnus albacares*), bigeye (*Thunnus obesus*) and skipjack tuna (*Katsuwonus pelamis*) were also considered. These catch data were used to ground truth the buoy's ability to detect the presence and size of tuna aggregations, assuming that the entire fish aggregation is encircled and captured by the fishing vessel. Conversely, newly deployed DFADs and visits to DFADs that did not result in any catch were used to ground truth the buoy's ability of detecting the absence of a tuna aggregation. For this assessment, DFAD deployments and visits where fishing sets were reported within the following week were omitted, to ensure that the data truly represented the absence of tuna at the DFADs. Similarly, only the deployments of new DFADs were considered and all other deployment operations were discarded (e.g., reinforcement of an existing DFAD, deployment of a buoy on a natural log).

Skunk fishing sets (sets where the tuna school totally or partially escaped) and activities, for which the reported set position was inconsistent with the position reported by the buoy, were removed. Only data for which the buoy identification code corresponded to a buoy code present

128 in the echosounder buoy database were retained in the analysis. The final database used for
129 each activity and ocean is described in Table 1.

130 2.2. Acoustic data pre-processing

131 Daily acoustic data provided by an individual buoy consists of a 50 × N matrix $\boldsymbol{S}$, where 50
132 represents the number of depth layers and N corresponds to the number of acoustic samples
133 provided for that day according to the operating mode of the buoy (in the default operating
134 mode, the acoustic scores are stored every 2 hours, thus N=12). Elements of the matrix $\boldsymbol{S}$
135 correspond to the daily acoustic scores S_{ij} (i.e., integers ranging between 0 and 7) recorded at
136 different depth layers i (i=1, 50) and different times of the day j (j=1, N). In a pre-processing
137 step, the temporal and spatial information was aggregated to standardize the data and achieve a
138 reduction in dimensions as follows:
139 (1) the acoustic scores of the two shallowest layers (0 – 6 m depth), representing the transducer
140 near-field, were removed, leading to a 48 × N matrix;
141 (2) for each layer i, the daily acoustic scores S_{ij} were averaged over 4-hours periods, resulting
142 in a reduced matrix $\boldsymbol{S'}$ of 48 × 6 (Fig. 2);
143 (3) a clustering method was applied on $\boldsymbol{S'}$ along the dimension i, to identify homogeneous
144 groups of depth layers. The clustering method was based on a dissimilarity matrix computed
145 from Euclidean distance and Ward's method (Murtagh and Legendre, 2014). The acoustic
146 scores in each identified group were compared through a Kruskal-Wallis test[1];
147 (4) for each homogeneous group G, the acoustic scores recorded previously for each of the i
148 depth layers constituting the group were summed and rescaled to obtain a unique score (S''_{Gj})
149 per group G and time period j, according to Eq. 1.

[1] Clustering analyses were conducted using the R function "*hclust*" (R Core Team, 2019), and the Kruskal-Wallis test with the R function "*kruskal.test*"

$$S''_{Gj} = \frac{\sum_{i=1}^{n_G} s'_{ij}}{maxs \times n_G} \qquad (1)$$

where j denotes the 4-hours time period, n_G the number of depth layers belonging to group G and *maxs* is a constant denoting the maximum score (7 in the case of M3I buoys). The result of the pre-processing step leads to a $N_G \times 6$ matrix $\boldsymbol{S''}$ (i.e., N_G groups of layers × 6 four-hour periods recorded during a day), summarizing the acoustic information collected on a daily scale, and referred to hereafter as a "daily acoustic matrix" (Fig. 2).

2.3. Supervised learning classification

2.3.1. Training dataset

The training datasets were constructed by cross-matching activity data (catch, deployments, visits without fishing sets) with the daily acoustic matrices, using buoy identification codes, dates and times for each ocean. A first binary training dataset was constructed for describing the presence or absence of tuna, in which catch events corresponded to tuna presence and deployment and visits without catch, to the absence of tuna (see Table 2). A second multiclass training dataset was created for describing the size of the tuna aggregation. The catch data were divided into three classes: < 10 tons, 10 – 25 tons, >25 tons, based on the total catch of the set (i.e., the sum of the catch of the three target tuna species: yellowfin tuna, bigeye tuna and skipjack tuna). The number and limits of the size classes were selected in order to retain a sufficient and balanced number of data points in each class for the learning process, while also maintaining consistency with the catch data. Class limits were based on the first quantile (10 tons) and the average (25 tons) of catches under DFADs in the dataset (see Table 3).

The daily acoustic matrices of tuna presence were constructed using the acoustic data recorded the day before catch events. Similarly, the daily acoustic matrices corresponding to tuna absence were selected from the daily acoustic matrices obtained the day prior to DFAD visits

without fishing sets, and those obtained on the fifth day after new DFAD deployments. The rationale for considering these 5-day periods after deployment was to account for the acoustic signal produced by the non-tuna species. Prior studies (Deudero et al., 1999; Castro et al., 2002; Nelson, 2003; Moreno et al., 2007; Macusi et al., 2017) have indicated that the colonization of DFADs by non-tuna species occurs within a range of a few hours to one week after deployment. Furthermore, preliminary analyses conducted on 528 and 5868 newly deployed DFADs, in the eastern Atlantic and western Indian oceans respectively, indicated a rapid increase in the acoustic signal recorded by the buoys during the first five days following deployment (Supplementary Appendix A3: Fig. A3.1 and A3.2). After considering all of these reasons, we assumed that acoustic data recorded at this post deployment time-scale were more likely to represent the presence of non-tuna species under DFADs.

2.3.2. Random forest algorithm

The random forest classification algorithm[2] (Breiman, 2001) was applied on an ocean-specific basis. Predictors were represented by daily acoustic matrix values. Three thousand trees were grown for each classification. This high value does not negatively impact the model's performance (Breiman, 2001), and helps to stabilize the importance of the variables more effectively (Liaw and Wiener, 2002; Probst et al., 2019). For each classification model, the number of variables randomly sampled as candidates at each split was assessed through a grid-search strategy implemented with the R package "caret" (Kuhn, 2008). In order to deal with the imbalanced number of observations in the different size categories a stratified down-sampling procedure, which consisted of resampling the dominant size categories to make their frequencies closer to the least common size category, was also applied (Kuhn and Johnson, 2013).

[2] The random forest classification was performed by using the R package "randomForest" (Liaw and Wiener, 2002)

196 2.3.3. Model evaluation

197 The overall accuracy (i.e., the proportion of correct predictions) and the kappa coefficient
198 (Cohen, 1968) were used to assess the overall performance of both binary and multi-size
199 category classifications. Kappa coefficient is a reliability index estimated according to Eq. 2:

200 $$kappa = \frac{Pr(a) - Pr(e)}{1 - Pr(e)} \qquad (2)$$

201 where *Pr(a)* is the total proportion of agreement between the observed and predicted classes
202 and *Pr(e)* is the theoretical proportion of agreement expected by chance. The closer this ratio
203 is to 1, the better the classification performed.

204 In each classification, the conventional statistical measures of the performance of a binary
205 classification test: sensitivity, specificity, and precision were evaluated from confusion
206 matrices, using Eq. 3 - 5:

207 $$Sensitivity = \frac{TP}{TP+FN} \qquad (3)$$

208 $$Specificity = \frac{TN}{FP+TN} \qquad (4)$$

209 $$Precision = \frac{TP}{TP+FP} \qquad (5)$$

210 where for presence/absence classification, *TP* (true positive) and *TN* (true negative) are the
211 proportions of presence (or absence) correctly classified; *FN* (false negative) and *FP* (false
212 positive) are the proportions of absence (or presence) incorrectly predicted. For multiclass
213 classification, positive cases correspond to the aggregation size category considered during the
214 evaluation, while all other categories correspond to negative cases. Sensitivity (also known as
215 recall or true positive rate) measures the efficiency of the algorithm in correctly classifying
216 positive cases, and specificity (or true negative rate) measures the efficiency of the algorithm

217 in correctly classifying negative cases. Precision (or positive predictive value) is the fraction of
218 correctly predicted presence among all tuna presence prediction.

219 The importance of the predictors in the classification process for each ocean was assessed
220 through the analysis of the mean decrease in accuracy of the random forest model (i.e., the
221 increase of prediction error after permuting each variable while all others remained unchanged
222 during the tree construction; Breiman, 2001). Model training and evaluation were performed
223 through a hold-out validation method which was repeated ten times. In each of the ten replicates,
224 the original dataset was divided into two subsets: the training set and the validation dataset
225 (representing 75% and 25% of the initial data, respectively).

226 **3. Results**

227 3.*1. Pre-processing of sampled depth layers*

228 The clustering analysis carried out on the 3 m depth layers led in both oceans to the formation
229 of six groups with similar layer compositions between the two oceans (Fig. 3). In each ocean,
230 the comparison of the acoustic scores between the identified groups showed highly significant
231 differences (*p-value* at Kruskal-Wallis test < 0.001 for both Indian and Atlantic Oceans). Scores
232 declined strongly with depth (Fig. 4). The deepest group of layers (which also aggregated the
233 greatest number of layers), exhibited the lowest acoustic values, with averages close to zero
234 (Fig. 4).

235 *3.2. Presence/absence classification*

236 The random forest algorithm performed well in discriminating between the presence and
237 absence of tuna, with an overall accuracy of 75 and 85% in the Atlantic and Indian oceans,
238 respectively (Table 4). In the Atlantic Ocean, the classification model was effective in detecting
239 DFAD aggregations with tuna (sensitivity of 0.83), but exhibited a notable level of false

positives (specificity of 0.67). In the Indian Ocean the opposite trend was observed with the classification of tuna presence performing well (sensitivity of 0.81) and the detection of their absence also producing reliable results (specificity of 0.90).

3.3. Classification of aggregation sizes

The classification of aggregations into size classes was considerably less efficient than the presence-absence classification, with low overall accuracies (48 and 47 %) observed for the Atlantic and the Indian Oceans, respectively (Table 5). In the Atlantic Ocean, the highest proportion of misclassification was observed in the 10 – 25 tons category (precision of 0.22), whereas tuna schools below 10 tons and above 25 tons both performed similarly (precision of 0.32 and 0.28 respectively). In the Indian Ocean, tuna schools over 25 tons and below 10 tons were also the most reliably detected aggregation size classes (precision of 0.44 and 0.42 respectively); while intermediate aggregation sizes (10 – 25 tons) were successfully classified less regularly (precision of 0.35).

3.4. Predictor importance

For both binary and multiclass classifications, the importance of the acoustic predictors in the classification process showed strong ocean-specific patterns. In the Atlantic Ocean, the detection of tunas was principally driven by acoustic data recorded from 6 m to 45 m (Fig. 5A and 6A). Conversely, in the Indian Ocean, the main predictors resulted from deeper layers (30 m to 150 m, Figure 5B and 6B). In these depth ranges, acoustic data recorded during daytime (4 am - 4 pm) appeared to be the most significant for both oceans and across all types of classifications. It should, however, be noted that in the Atlantic Ocean, the binary classification produced a wider time window (0 to 4 pm) than in the Indian Ocean.

4. Discussion

This study describes a new methodology for processing data collected by a commercial echosounder buoy commonly used in the DFAD purse seine fishery. The approach utilizes the acoustic scores (reflective of abundance) recorded at different depths and times of the day and combines data pre-processing procedures and machine learning algorithms to classify tropical tuna aggregations under DFADs. Although several models of echosounder buoys process data internally and generate abundance indices for tuna, previous studies have shown that such information can be unreliable (Lopez et al., 2014, 2016). This could explain why most purse seine skippers pay little attention to this information. Rather than relying solely on these processed outputs, skippers tend to combine the acoustic information recorded at specific depths and times with their empirical knowledge and the oceanographic characteristics of the region to assist their decision making.

Working on a different brand of buoy, Lopez et al. (2016) developed the first approach to improve biomass estimations from data collected by echosounder buoys. These authors suggested that the acoustic signal collected during sunrise (i.e., when tuna are generally the most tightly concentrated under DFADs), should be considered for processing and assumed the structure of the aggregated biomass based on knowledge of the vertical behaviour of species under floating objects. Under this assumption, they suggested a vertical segregation between the species that make up the multispecific aggregation under DFADs (non-tuna species [3 – 25 m], small tunas [25 – 80 m] and large tunas [80 – 115 m]), and applied an echo-integration procedure to convert the acoustic signal from each depth layer into biomass estimates using specific values of target strength and individual average weight for each group. The application of this approach to a larger dataset in the Indian Ocean (287 fishing sets) by Orue et al (2019) was found to be less effective than expected, and potentially affected by the large spatio-

287 temporal variability between oceanic regions which skewed the main assumptions that underlie
288 the approach.

289 The methodology used by this study did not make any assumptions regarding the vertical and
290 temporal distribution of tuna at DFADs. Using a supervised learning algorithm, this
291 methodology mimics the learning process of the fishers on how they interpret the acoustic
292 scores based on their experience. The training dataset used for this purpose utilizes buoy data,
293 which is considered to be ground-truthed. These ground-truthed data have three underlying
294 assumptions. The first assumption is that the tuna caught by a purse seine vessel around a DFAD
295 represents all the tuna aggregated under that DFAD. This is typically the case, although it is
296 possible that some tuna escape during the fishing procedure, such events are considered to be
297 minor (Muir et al., 2012). In exceptional situations when very large fishing sets are made (>
298 200 t), the skipper may decide to retain only part of the aggregation to avoid damaging the net.
299 The second assumption is that tunas do not immediately associate with newly deployed DFADs.
300 Although Orue et al. (2019b) indicated that tuna may arrive first under DFADs, previous studies
301 (Deudero et al., 1999; Castro et al., 2002; Nelson, 2003; Macusi et al., 2017), including
302 interviews with fishers (Moreno et al., 2007) suggested otherwise. In this study, the daily
303 acoustic matrix recorded five days after the deployment of a new DFAD was used to represent
304 the absence of tuna. It would be useful to develop dedicated studies that would aid in the
305 understanding of the aggregation process of tuna and non-tuna species around DFADs. Finally,
306 the third assumption considered that a purse seine vessel visiting its own DFAD (DFAD
307 equipped with the vessel's buoy) without fishing also represents the absence of a tuna
308 aggregation at the DFAD. It may be countered that a skipper could decide not to set on a DFAD
309 when the vessel is already full, but this is an extremely rare event. External factors (e.g. strong
310 currents) may also impede the fishing operations. However, if a vessel heads towards a DFAD
311 that it owns, it is fair to assume that this would result in a fishing set (if tunas are present).

312 Furthermore, in an effort to avoid any bias associated with the external factors that could
313 influence the skipper's decision, only DFAD visits that were not followed by a fishing set within
314 seven days were taken into consideration. Our decision to include visits without fishing
315 operations in the training database as "absence of tuna" was taken based on numerous
316 discussions with skippers. According to many of them, it is not uncommon that the echosounder
317 buoys report high levels of acoustic energy even if tuna are absent from the aggregation. The
318 objective of including these DFAD visits in the database was to improve the ability of the
319 classification model to detect such false positives.

320 The results from this study highlight the effectiveness of the proposed methodology for
321 discriminating between the presence and absence of tuna aggregations under DFADs equipped
322 with M3I buoys in both the Indian and Atlantic oceans. To date the reliability of this model of
323 buoy in estimating the presence and size of tuna aggregations had only been assessed
324 anecdotally based on opinion and feedback from skippers. The development of reliable methods
325 for processing data provided by commercial echosounder buoys represents a key step in the use
326 of these fishing tools for scientific purposes, particularly the study of the different aspects of
327 the ecology and behaviour of tuna associated with floating objects. The algorithm's lower
328 performance in the Atlantic Ocean, where a higher proportion of false positive predictions of
329 tuna presence were generated, could well be related to the size of the training dataset. In the
330 Atlantic Ocean, this dataset was 5.5 times smaller than that used for the India Ocean. However,
331 this difference may also reflect an ocean-specific vertical distribution of fish aggregations under
332 DFADs. In the Indian Ocean, previous studies have described a vertical segregation between
333 tuna and non-tuna species (Forget et al., 2015; Macusi et al., 2017). Such segregation would
334 result in the determination of an absence of tuna to be straightforward for the classification
335 algorithm. To date no studies have investigated the vertical distribution of tuna and non-tuna
336 species under DFADs in the Atlantic Ocean. The depth of the thermocline in the eastern Atlantic

337 Ocean is known to be shallower than in the western Indian Ocean (Schott et al., 2009; Xie and
338 Carton, 2013). This difference may result in tunas occupying shallower depths and thus mixing
339 more regularly with non-tuna species. Such a phenomenon could provide an explanation for the
340 higher rates of false positives generated in the Atlantic Ocean (i.e., false detection of the
341 presence of tuna). The analysis of the relevance of the predictive factors in the random forest
342 classifications showed that, for both oceans, daytime periods were the most relevant factor for
343 distinguishing the presence of tuna schools from other acoustic targets. This result is likely
344 linked to the behaviour of tuna schools and their spatial and temporal distribution around
345 DFADs. Sonar surveys conducted on DFADs in the Indian Ocean revealed that tuna form a
346 large number of small and dispersed schools during the night, and few and larger schools during
347 daytime (Trygonis et al., 2016). Another possible reason could be related to the influence of the
348 diel vertical migration of the deep scattering layer to the near surface at night (Robinson and
349 Goómez-Gutieérrez, 1998), which may affect the acoustic signal.

350 In both oceans, the performance of the classification algorithm for discriminating between
351 different aggregation sizes was considerably less satisfactory than the presence/absence of
352 tunas. There are several possible explanations for these limitations. One potential source of bias
353 may stem from the differing species composition considered in each size class. Due to skipjack
354 tuna lacking a swim bladder, their acoustic response is very different from that of yellowfin or
355 bigeye tuna (Josse and Bertrand 2000; Boyra et al. 2018), as such an aggregation of a given size
356 would result in different acoustic signatures depending on the percentage of each species that
357 make it up. Another source of bias could be linked to the position of the tuna aggregation in
358 relation to the area that is sampled by the buoy (detection cone). Depending on the size of the
359 aggregation and the behaviour of tuna around the DFAD, it is likely that the buoy's acoustic
360 cone only detects part of the tuna aggregation, especially at shallow depths. Some
361 environmental factors could also affect both the acoustic signal detection and fish behaviour,

362 and could thus have an effect on the classification of the aggregation size. Water temperature,
363 for example, is known to have an effect on both the acoustic signal (Bamber and Hill, 1979;
364 Straube and Arthur, 1994) and the abundance of tuna (Boyce et al., 2008). As such, the
365 interpretation of buoy data, particularly concerning the accurate estimation of the aggregated
366 biomass, may be strongly influenced by area and season-specific factors. In addition, close
367 examination of the scores in the layer groups identified by the cluster analysis also revealed that
368 layers deeper than 50 m were characterized by very low scores (Fig. 4). Previous studies on the
369 vertical distribution of fish species under DFADs found that tuna regularly occurred below this
370 depth (Dagorn et al. 2007a; Dagorn et al. 2007b; Forget et al. 2015; Matsumoto et al. 2016;
371 Lopez et al., 2017). Consequently, it appears fair to assume that the low values obtained for
372 these depths are likely related to the limited detection capability of the device at such depths,
373 which may also explain the poor estimates of the size of the tuna schools.

374 The principle findings of this work showed that machine learning offers promising pathways
375 for processing acoustic data provided by commercial echosounder buoys. Although this work
376 has focused on a single model of buoy, it can easily be expanded to encompass other models
377 and brands. The only essential requirement is access to a large training database.

378 **5. Conclusion**

379 The methodology developed in this study provides an indicator of presence/absence of tuna
380 schools at DFADs in both the Atlantic and Indian Oceans, from simplified acoustic data
381 collected by one of the echosounder buoy models used in the tuna purse seine fishery. This
382 approach has the potential to summarize and analyse a large amount of acoustic data, with an
383 efficiency that obviously depends on the nature and quality of the data provided. Nevertheless,
384 the rapid and continuous evolution in echosounder buoys technology observed since their
385 introduction is likely to provide, over time, better and more detailed data, leading to a

substantial improvement in the performance of the proposed methodology, specifically regarding assessment of aggregation sizes under DFADs. Applying this approach to other echosounder buoy models, like new multi-frequency buoy models, widely adopted in recent years, could also allow to assess and compare buoy reliabilities. Finally, although the availability of more extensive databases (with matched acoustic and catch data) and more detailed acoustic data (beyond the discrete 0 – 7 acoustic indices) could improve this methodology, the accurate discrimination between the presence and absence of tuna schools around DFADs obtained in this study constitutes a critical step towards the exploitation of echosounder buoy data for providing novel and robust indicators of abundance for the management of FAD fisheries in years to come.

6. Acknowledgements

This project was co-funded by "Observatoire des Ecosystèmes Pélagiques Tropicaux exploités" (Ob7) from IRD/MARBEC and by the ANR project BLUEMED (ANR-14-ACHN-0002). The authors are grateful to ORTHONGEL and its contracting parties (CFTO, SAPMER, SAUPIQUET) for providing the echosounder buoys data. The authors also thank all the skippers who gave their time to share their experience and knowledge on the echosounder buoys. The authors sincerely thank the contribution of the staff of the Ob7 for their work on the databases of the echosounder buoys and observer data. We are also sincerely grateful to the buoy manufacturers for their useful advice and information on their echosounder buoys.

406 **References**

407 Albert, J.A., Beare, D., Schwarz, A.M., Albert, S., Warren, R., Teri, J., Siota, F., Andrew,
408 N.L., 2014. The contribution of nearshore fish aggregating devices (FADs) to food
409 security and livelihoods in Solomon Islands. *PLoS One* 9.
410 https://doi.org/10.1371/journal.pone.0115386

411 Baidai, Y., Capello, M., Billet, N., Floch, L., Simier, M., Sabarros, P., Dagorn, L., 2017.
412 Towards the derivation of fisheries-independent abundance indices for tropical tunas:
413 Progress in the echosounders buoys data analysis. IOTC-2017-WPTT19-22.

414 Bamber, J.C., Hill, C.R., 1979. Ultrasonic attenuation and propagation speed in mammalian
415 tissues as a function of temperature. *Ultrasound Med. Biol.* 5, 149–157.
416 https://doi.org/10.1016/0301-5629(79)90083-8

417 Bosch, P., López, J., Ramírez, H., Robotham, H., 2013. Support vector machine under
418 uncertainty: An application for hydroacoustic classification of fish-schools in Chile.
419 *Expert Syst. Appl.* 40, 4029–4034.
420 https://doi.org/https://doi.org/10.1016/j.eswa.2013.01.006

421 Boyce, D., Tittensor, D., Worm, B., 2008. Effects of temperature on global patterns of tuna
422 and billfish richness. *Mar. Ecol. Prog. Ser.* 355, 267–276.
423 https://doi.org/10.3354/meps07237

424 Boyra, G., Moreno, G., Sobradillo, B., Pérez-Arjona, I., Sancristobal, I., Demer, D.A., 2018.
425 Target strength of skipjack tuna (*Katsuwonus pelamis*) associated with fish aggregating
426 devices (FADs). *ICES J. Mar. Sci.* 75, 1790–1802.
427 https://doi.org/10.1093/icesjms/fsy041

428 Brehmer, P., Sancho, G., Trygonis, V., Itano, D., Dalen, J., Fuchs, A., Faraj, A., Taquet, M.,
429 2018. Towards an Autonomous Pelagic Observatory: Experiences from Monitoring Fish
430 Communities around Drifting FADs. *Thalass. An Int. J. Mar. Sci.* 35, 177–189.
431 https://doi.org/10.1007/s41208-018-0107-9

432 Breiman, L., 2001. Random forests. *Mach. Learn.* 45, 5–32.
433 https://doi.org/10.1023/A:1010933404324

434 Capello, M., Deneubourg, J.L., Robert, M., Holland, K.N., Schaefer, K.M., Dagorn, L., 2016.
435 Population assessment of tropical tuna based on their associative behavior around

436 floating objects. *Sci. Rep*. 6, 1–14. https://doi.org/10.1038/srep36415

437 Castro, J.J., Santiago, J. a, Santana-Ortega, a T., 2002. A general theory on fish aggregation
438 to floating objects: An alternative to the meeting point hypothesis. *Rev. Fish Biol. Fish*.
439 11, 255–277. https://doi.org/10.1023/A:1020302414472

440 Cohen, J., 1968. Weighted kappa: Nominal scale agreement provision for scaled disagreement
441 or partial credit. *Psychol. Bull*. 70, 213–220. https://doi.org/10.1037/h0026256

442 Dagorn, L., Holland, K.N., Itano, D.G., 2007a. Behavior of yellowfin (*Thunnus albacares*)
443 and bigeye (*T. obesus*) tuna in a network of fish aggregating devices (FADs). *Mar. Biol*.
444 151, 595–606. https://doi.org/10.1007/s00227-006-0511-1

445 Dagorn, L., Pincock, D., Girard, C., Holland, K., Taquet, M., Sancho, G., Itano, D.,
446 Aumeeruddy, R., 2007b. Satellite-linked acoustic receivers to observe behavior of fish in
447 remote areas. *Aquat. Living Resour*. 20, 307–312. https://doi.org/10.1051/alr:2008001

448 Dagorn, L., Holland, K.N., Restrepo, V., Moreno, G., 2013. Is it good or bad to fish with
449 FADs? What are the real impacts of the use of drifting FADs on pelagic marine
450 ecosystems? *Fish Fish*. 14, 391–415. https://doi.org/10.1111/j.1467-2979.2012.00478.x

451 Davies, T.K., Mees, C.C., Milner-Gulland, E.J., 2014. The past, present and future use of
452 drifting fish aggregating devices (FADs) in the Indian Ocean. *Mar. Policy* 45, 163–170.
453 https://doi.org/10.1016/j.marpol.2013.12.014

454 Deudero, S., Merella, P., Massutí, E., Alemany, F., 1999. Fish communities associated with
455 FADs. *Sci. Mar*. 63, 199–207.

456 Fernandes, P.G., 2009. Classification trees for species identification of fish-school echotraces.
457 *ICES J. Mar. Sci*. 66, 1073–1080. https://doi.org/10.1093/icesjms/fsp060

458 Filmalter, J.D., Dagorn, L., Cowley, P.D., Taquet, M., 2011. First Descriptions of the
459 Behavior of Silky Sharks, *Carcharhinus Falciformis*, Around Drifting Fish Aggregating
460 Devices in the Indian Ocean. *Bull. Mar. Sci*. 87, 325–337.
461 https://doi.org/10.5343/bms.2010.1057

462 Fonteneau, A., Chassot, E., Bodin, N., 2013. Global spatio-temporal patterns in tropical tuna
463 purse seine fisheries on drifting fish aggregating devices (DFADs): Taking a historical
464 perspective to inform current challenges. *Aquat. Living Resour*. 26, 37–48.
465 https://doi.org/10.1051/alr/2013046

Fonteneau, A., Chassot, E., Gaertner, D., 2015. Managing tropical tuna purse seine fisheries through limiting the number of drifting fish aggregating devices in the Atlantic: food for thought. *Collect. Vol. Sci. Pap. ICCAT*, 71(1), 460-475.

Fonteneau, A., Gaertner, D., Nordstrom, V., 1999. An overview of problems in the CPUE-abundance relationship for the tropical purse seine fisheries. *Collect. Vol. Sci. Pap. ICCAT* 49, 259–276.

Fonteneau, A., Gascuel, D., Pallarés, P., 1998. Vingt-cinq ans d'évaluation des ressources thonières de l'Atlantique : Quelques réflexions methodologiques. *Collect. Vol. Sci. Pap. ICCAT* 50, 523–561.

Forget, F.G., Capello, M., Filmalter, J.D., Govinden, R., Soria, M., Cowley, P.D., Dagorn, L., 2015. Behaviour and vulnerability of target and non-target species at drifting fish aggregating devices (FADs) in the tropical tuna purse seine fishery determined by acoustic telemetry. *Can. J. Fish. Aquat. Sci*. 72, 1398–1405. https://doi.org/10.1139/cjfas-2014-0458

Gaertner, D., Ariz, J., Bez, N., Clermidy, S., Moreno, G., Murua, H., Soto, M., 2015. Catch, effort, and ecosystem impacts of fad-fishing (CECOFAD). *Collect. Vol. Sci. Pap. ICCAT* 71, 525–539.

Goujon, M., Maufroy, A., Relot-Stirnemann, A., Moëc, E., Bach, P., Cauquil, P., and Sabarros, P., 2017. Collecting data on board French tropical tuna purse seiners with common observers: results of ORTHONGEL's voluntary observer program OCUP in the Atlantic Ocean (2013-2017). IOTC-2017-WPDCS-22.

Goujon, M., Maufroy, A., Cauquil, P., Sabarros, P., and Bach, P., 2018. Collecting data on board French tropical tuna purse seiners with common observers: results of ORTHONGEL's voluntary observer program ocup in the Atlantic Ocean (2013-2017). *Collect. Vol. Sci. Pap. ICCAT* 74, 3784–3805.

Govinden, R., Jauhary, R., Filmalter, J., Forget, F., Soria, M., Adam, S., Dagorn, L., 2013. Movement behaviour of skipjack (*Katsuwonus pelamis*) and yellowfin (*Thunnus albacares*) tuna at anchored fish aggregating devices (FADs) in the Maldives, investigated by acoustic telemetry. *Aquat. Living Resour*. 26, 69–77. https://doi.org/10.1051/alr/2012022

Josse, E., Bertrand, A., 2000. In situ acoustic target strength measurements of tuna associated

with a fish aggregating device. *ICES J. Mar. Sci*. 57, 911–918. https://doi.org/10.1006/jmsc.2000.0578

Kakuma, S., 2001. Synthesis on moored FADs in the North West Pacific region. *Actes Colloq. IFREMER* 63–77.

Kuhn, M., 2008. Building Predictive Models in R Using the caret Package. *J. Stat. Softw*. 28, 1–26. https://doi.org/10.1053/j.sodo.2009.03.002

Kuhn, M., Johnson, K., 2013. Applied Predictive Modeling, Applied Predictive Modeling. Springer New York, New York, NY. https://doi.org/10.1007/978-1-4614-6849-3

Lennert-Cody, C.E., Hall, M.A., 2001. The development of the purse seine fishery on drifting Fish Aggregating Devices in the eastern Pacific Ocean: 1992-1998. *Actes Colloq. IFREMER* 78–107.

Liaw, A., Wiener, M., 2002. Classification and regression by randomForest. *R news* 2, 18–22. https://doi.org/10.1177/154405910408300516

Lopez, J., Moreno, G., Boyra, G., Dagorn, L., 2016. A model based on data from echosounder buoys to estimate biomass of fish species associated with fish aggregating devices. *Fish. Bull.* 114, 166–178. https://doi.org/10.7755/FB.114.2.4

Lopez, J., Moreno, G., Ibaibarriaga, L., Dagorn, L., 2017. Diel behaviour of tuna and non-tuna species at drifting fish aggregating devices (DFADs) in the Western Indian Ocean, determined by fishers' echo-sounder buoys. *Mar. Biol.* 164, 44. https://doi.org/10.1007/s00227-017-3075-3

Lopez, J., Moreno, G., Sancristobal, I., Murua, J., 2014. Evolution and current state of the technology of echo-sounder buoys used by Spanish tropical tuna purse seiners in the Atlantic, Indian and Pacific Oceans. *Fish. Res*. 155, 127–137. https://doi.org/10.1016/j.fishres.2014.02.033

Macusi, E.D., Abreo, N.A.S., Babaran, R.P., 2017. Local Ecological Knowledge (LEK) on Fish Behavior Around Anchored FADs: the Case of Tuna Purse Seine and Ringnet Fishers from Southern Philippines. *Front. Mar. Sci*. 4, 1–13. https://doi.org/10.3389/fmars.2017.00188

Malfante, M., Mars, J.I., Dalla Mura, M., Gervaise, C., 2018. Automatic fish sounds classification. *J. Acoust. Soc. Am.* 143, 2834–2846. https://doi.org/10.1121/1.5036628

527 Matsumoto, T., Satoh, K., Semba, Y., Toyonaga, M., 2016. Comparison of the behavior of
528 skipjack (*Katsuwonus pelamis*), yellowfin (*Thunnus albacares*) and bigeye (*T. obesus*)
529 tuna associated with drifting FADs in the equatorial central Pacific Ocean. *Fish.*
530 *Oceanogr.* 25, 565–581. https://doi.org/10.1111/fog.12173

531 Maufroy, A., Kaplan, D.M., Bez, N., De Molina, A.D., Murua, H., Floch, L., Chassot, E.,
532 2017. Massive increase in the use of drifting Fish Aggregating Devices (dFADs) by
533 tropical tuna purse seine fisheries in the Atlantic and Indian Oceans. *ICES J. Mar. Sci.*
534 74, 215–225. https://doi.org/10.1093/icesjms/fsw175

535 Maunder, M.N., Sibert, J.R., Fonteneau, A., Hampton, J., Kleiber, P., Harley, S.J., 2006.
536 Interpreting catch per unit effort data to assess the status of individual stocks and
537 communities. *ICES J. Mar. Sci*. 63, 1373–1385.
538 https://doi.org/10.1016/j.icesjms.2006.05.008

539 Mitsunaga, Y., Endo, C., Anraku, K., Selorio, C.M., Babaran, R.P., 2012. Association of early
540 juvenile yellowfin tuna *Thunnus albacares* with a network of payaos in the Philippines.
541 *Fish. Sci*. 78, 15–22. https://doi.org/10.1007/s12562-011-0431-y

542 Moreno, G., Boyra, G., Sancristobal, I., Itano, D., Restrepo, V., 2019. Towards acoustic
543 discrimination of tropical tuna associated with Fish Aggregating Devices. *PLoS One* 14,
544 e0216353. https://doi.org/10.1371/journal.pone.0216353

545 Moreno, G., Dagorn, L., Capello, M., Lopez, J., Filmalter, J., Forget, F., Sancristobal, I.,
546 Holland, K., 2016. Fish aggregating devices (FADs) as scientific platforms. *Fish. Res.*
547 178, 122–129. https://doi.org/10.1016/j.fishres.2015.09.021

548 Moreno, G., Dagorn, L., Sancho, G., Itano, D., 2007. Fish behaviour from fishers' knowledge:
549 the case study of tropical tuna around drifting fish aggregating devices (DFADs). *Can. J.*
550 *Fish. Aquat. Sci.* 64, 1517–1528. https://doi.org/10.1139/f07-113

551 Muir, J., Itano, D., Hutchinson, M., Leroy, B., Holland, K., 2012. Behavior of target and non-
552 target species on drifting FADs and when encircled by purse seine gear. *West. Cent.*
553 *Pacific Fish. Commision - Sci. Comm*. 8 8 pp.

554 Murtagh, F., Legendre, P., 2014. Ward's Hierarchical Agglomerative Clustering Method:
555 Which Algorithms Implement Ward's Criterion? *J. Classif.* 31, 274–295.
556 https://doi.org/10.1007/s00357-014-9161-z

557 Nelson, P.A., 2003. Marine fish assemblages associated with fish aggregating devices
558 (FADs): Effects of fish removal, FAD size, fouling communities, and prior recruits. *Fish.*
559 *Bull.* 101, 835–850.

560 Noda, J.J., Travieso, M.C., Sánchez-Rodríguez, D., Travieso, C.M., Sánchez-Rodríguez, D.,
561 2016. Automatic Taxonomic Classification of Fish Based on Their Acoustic Signals.
562 *Appl. Sci.* 6, 443. https://doi.org/10.3390/app6120443

563 Orue, B., Lopez, J., Moreno, G., Santiago, J., Boyra, G., Soto, M., Murua, H., 2019a. Using
564 fishers' echo-sounder buoys to estimate biomass of fish species associated with drifting
565 fish aggregating devices in the Indian Ocean. *Rev. Investig. Mar. AZTI* 26, 1–13.

566 Orue, B., Lopez, J., Moreno, G., Santiago, J., Soto, M., Murua, H., 2019b. Aggregation
567 process of drifting fish aggregating devices (DFADs) in the Western Indian Ocean: Who
568 arrives first, tuna or non-tuna species? *PLoS One* 14, e0210435.
569 https://doi.org/10.1371/journal.pone.0210435

570 Probst, P., Wright, M.N., Boulesteix, A.L., 2019. Hyperparameters and tuning strategies for
571 random forest. *Wiley Interdiscip. Rev. Data Min. Knowl. Discov*. 9(3), 1-15.
572 https://doi.org/10.1002/widm.1301

573 R Core Team, 2019. R: A language and environment for statistical computing. R Found Stat
574 Comput. https://www.R-project.org/

575 Robinson, C.J., Goómez-Gutieérrez, J., 1998. Daily vertical migration of dense deep
576 scattering layers related to the shelf-break area along the northwest coast of Baja
577 California, Mexico. *J. Plankton Res.* 20, 1679–1697.
578 https://doi.org/10.1093/plankt/20.9.1679

579 Robotham, H., Bosch, P., Gutiérrez-Estrada, J.C., Castillo, J., Pulido-Calvo, I., 2010.
580 Acoustic identification of small pelagic fish species in Chile using support vector
581 machines and neural networks. *Fish. Res.* 102, 115–122.
582 https://doi.org/https://doi.org/10.1016/j.fishres.2009.10.015

583 Roch, M.A., Soldevilla, M.S., Hoenigman, R., Wiggins, S.M., Hildebrand, J.A., 2008.
584 Comparison of machine learning techniques for the classification of echolocation clicks
585 from three species of odontocetes. *Can. Acoust*. 36(1), 41–47.

586 Santiago, J., Lopez, J., Moreno, G., Quincoces, I., Soto, M., Murua, H., 2016. Towards a

587 Tropical Tuna Buoy-derived Abundance Index (TT-BAI). *Collect. Vol. Sci. Pap. ICCAT*
588 72, 714–724.

589 Schott, F.A., Xie, S.P., McCreary, J.P., 2009. Indian Ocean circulation and climate variability.
590 *Rev. Geophys*. 47, 1–46. https://doi.org/10.1029/2007RG00024

591 Straube, W.L., Arthur, R.M., 1994. Theoretical estimation of the temperature dependence of
592 backscattered ultrasonic power for noninvasive thermometry. *Ultrasound Med. Biol*. 20,
593 915–922. https://doi.org/10.1016/0301-5629(94)90051-5

594 Taquet, M., Dagorn, L., Gaertner, J.-C., Girard, C., Aumerruddy, R., Sancho, G., Itano, D.,
595 2007. Behavior of dolphinfish (*Coryphaena hippurus*) around drifting FADs as observed
596 from automated acoustic receivers. *Aquat. Living Resour*. 20, 323–330.
597 https://doi.org/10.1051/alr:2008008

598 Torres-Irineo, E., Gaertner, D., Chassot, E., Dreyfus-León, M., 2014. Changes in fishing
599 power and fishing strategies driven by new technologies: The case of tropical tuna purse
600 seiners in the eastern Atlantic Ocean. *Fish. Res*. 155, 10–19.
601 https://doi.org/10.1016/j.fishres.2014.02.017

602 Trygonis, V., Georgakarakos, S., Dagorn, L., Brehmer, P., 2016. Spatiotemporal distribution
603 of fish schools around drifting fish aggregating devices. *Fish. Res*. 177, 39–49.
604 https://doi.org/10.1016/j.fishres.2016.01.013

605 Uranga, J., Arrizabalaga, H., Boyra, G., Hernandez, M.C., Goñi, N., Arregui, I., Fernandes,
606 J.A., Yurramendi, Y., Santiago, J., 2017. Detecting the presence-Absence of bluefin tuna
607 by automated analysis of medium-range sonars on fishing vessels. *PLoS One* 12, 1–18.
608 https://doi.org/10.1371/journal.pone.0171382

609 Xie, S.-P., Carton, J.A., 2013. Tropical Atlantic Variability: Patterns, Mechanisms, and
610 Impacts, in: Earth Climate: The Ocean-Atmosphere Interaction, Geophys. Monogr. pp.
611 121–142. https://doi.org/10.1029/147GM07

612 Zaugg, S., van der Schaar, M., Houégnigan, L., Gervaise, C., André, M., 2010. Real-time
613 acoustic classification of sperm whale clicks and shipping impulses from deep-sea
614 observatories. *Appl. Acoust*. 71, 1011–1019.
615 https://doi.org/https://doi.org/10.1016/j.apacoust.2010.05.005

616

Tables

Table 1: Number of fishing sets (with catch ≥ 1 ton), visit and deployment data collected from 2013-2018 and used in the presence-absence classification for the Atlantic and Indian Oceans.

	Atlantic Ocean			Indian Ocean		
	Catch	Visit	Deployment	Catch	Visit	Deployment
Logbook	817	255	405	2918	1031	6722
Observers	151	0	228	513	0	2487
Total	968	255	633	3431	1031	9209

Table 2: Structure of the training dataset used in the presence-absence and multiclass classification for the Atlantic and Indian Oceans (over the period 2013-2018).

Ocean	No tuna	Tuna		
		< 10 tons	[10, 25 tons]	> 25 tons
Atlantic	888	397	303	268
Indian	10240	904	1288	1239

Table 3: Summary statistics of major tuna catches (in tons) from DFAD fishing operations collected from observer and logbook databases from 2013 to 2018, in the Atlantic and Indian Oceans. (Min. and Max. denote for minimum and maximum catch values, respectively. SD represents standard deviation and Qu. stands for quantile)

Ocean	Min.	1st Qu.	Median	Mean	3rd Qu.	Max.	SD
Atlantic	1	6	15	22.61	30	177.70	25.59
Indian	1	10	20	26.73	34	300	26.77

629 Table 4: Summary of tuna presence/absence classification performances for the Atlantic and
630 Indian Oceans: mean and standard deviation values (in brackets) of evaluation metrics.

Evaluation Metrics	Atlantic	Indian
Accuracy	0.75 (0.02)	0.85 (0.01)
Kappa	0.51 (0.04)	0.70 (0.02)
Sensitivity	0.83 (0.02)	0.81 (0.01)
Specificity	0.67 (0.03)	0.90 (0.01)
Precision	0.73 (0.03)	0.88 (0.01)

631

632 Table 5: Summary of multiclass classification performances for the Atlantic and Indian Ocean. Mean and standard deviation (in brackets) of
633 evaluation metrics

	Atlantic Ocean				Indian Ocean			
	No tuna	<10 tons	[10 , 25 tons]	> 25 tons	No tuna	<10 tons	[10 , 25 tons]	> 25 tons
Sensitivity	0.67 (0.03)	0.36 (0.05)	0.24 (0.08)	0.34 (0.06)	0.87 (0.03)	0.19 (0.01)	0.29 (0.02)	0.54 (0.04)
Specificity	0.82 (0.02)	0.80 (0.03)	0.84 (0.04)	0.85 (0.04)	0.80 (0.01)	0.91 (0.01)	0.82 (0.02)	0.77 (0.01)
Precision	0.77 (0.03)	0.32 (0.04)	0.22 (0.04)	0.28 (0.05)	0.59 (0.02)	0.42 (0.04)	0.35 (0.03)	0.44 (0.02)
Accuracy	0.48 (0.02)				0.47 (0.02)			
Kappa	0.26 (0.03)				0.30 (0.02)			

634

Figures

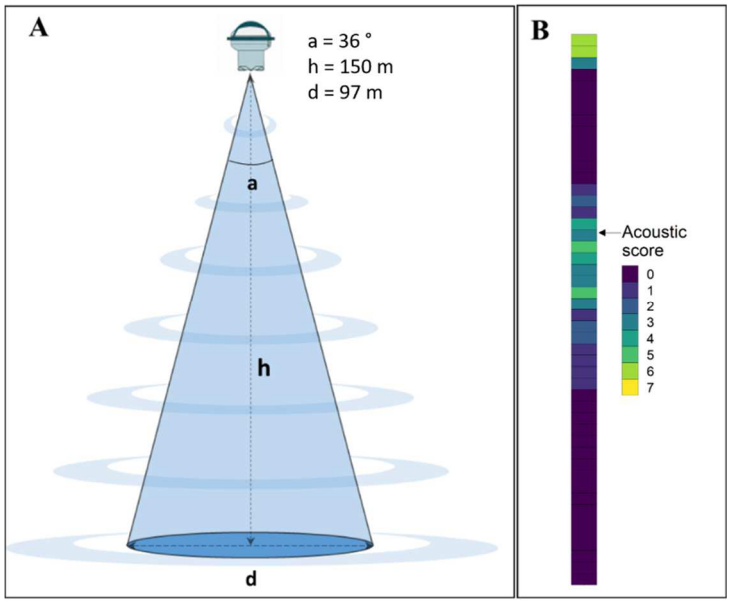

Fig. 1: Technical specifications of the Marine Instruments M3I echosounder buoy. (A): beam width or cover angle (a), depth range (h), and diameter (D) at 150 m, (B): example of an acoustic sample

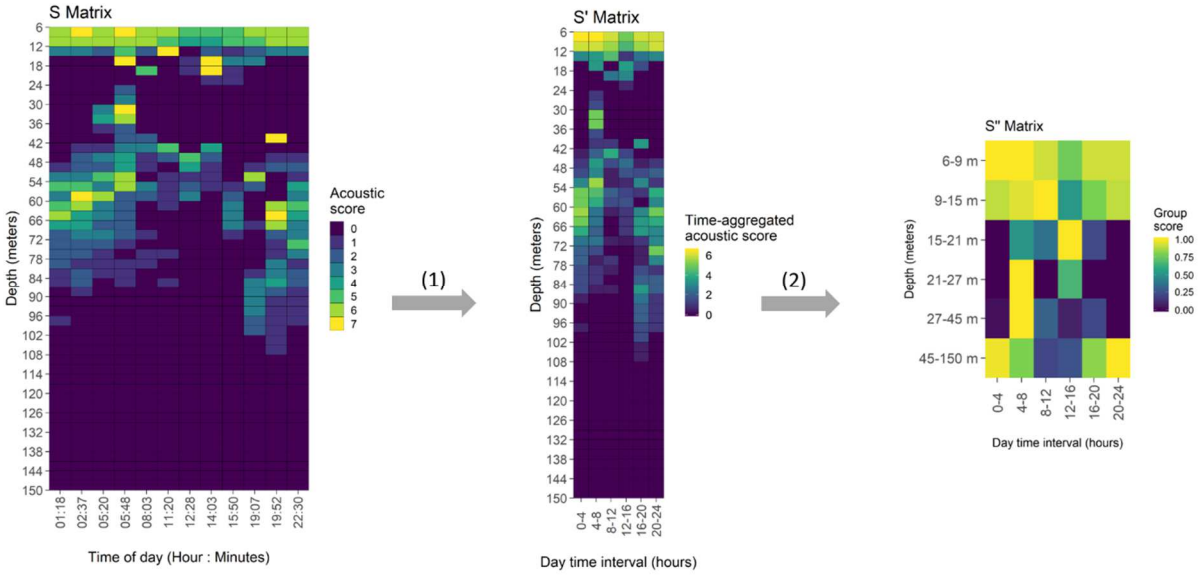

Fig. 2 : Schematic view of the acoustic data pre-processing. (1) Temporal resolution reduction, averaging acoustic samples over a 4-hour period. (2) Layer aggregation combining the 48 vertical layers into 6 layers based on cluster analysis. The final output is a 6×6 matrix summarizing the acoustic signal recorded over 24 hours between 6 and 150 m. Acoustic scores

645 are integer values (ranging from 0 to 7), representing the intensity of the acoustic backscattered
646 signal per 3 m depth layer. Time-aggregated acoustic scores represent the average value of the
647 acoustic scores over the 4-hour interval. Group scores represent the sum of layer scores (scaled
648 between 0 and 1) per homogeneous group of layers identified from the clustering analysis.

649

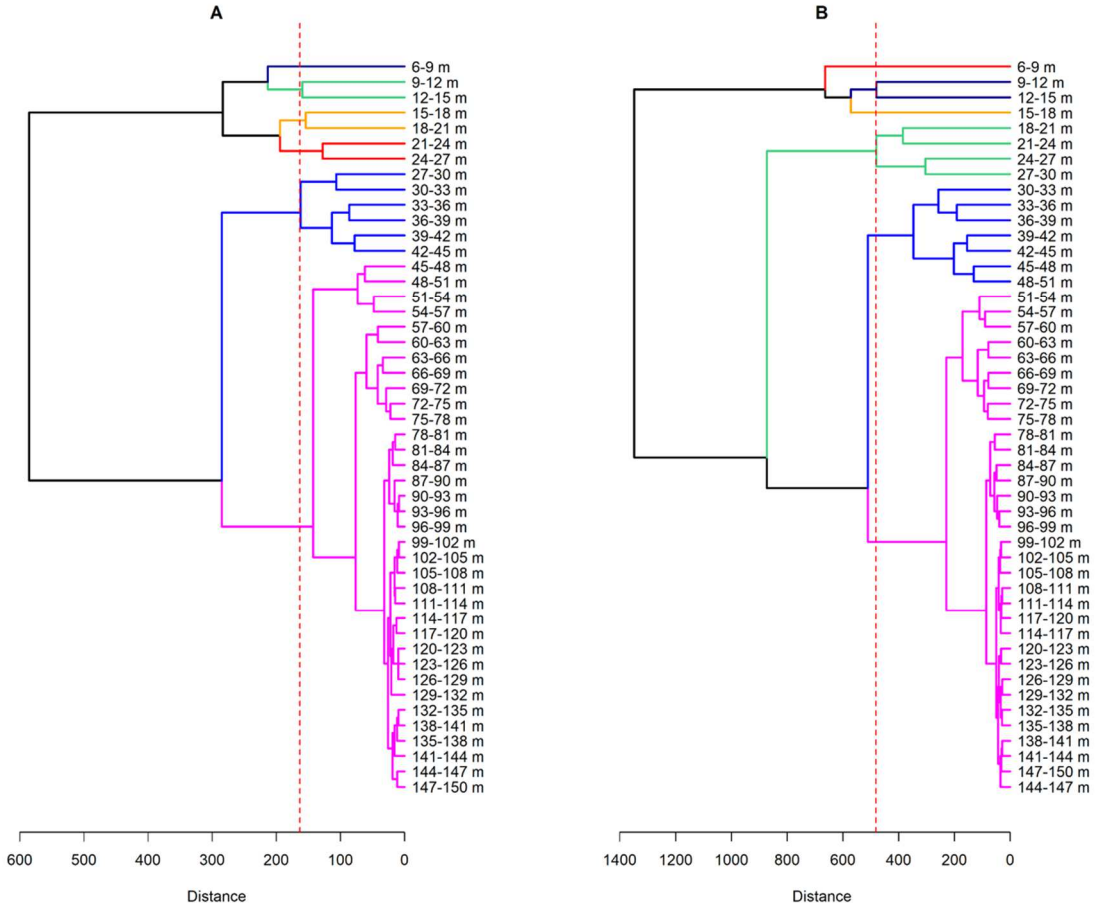

650

651 Fig. 3: Dendrogram from the cluster analysis of raw acoustic data for the Atlantic (A) and Indian
652 (B) Oceans. The red horizontal line indicates the height at which the dendrogram was sliced to
653 create the 6 groups of layers. Colors identify the different groups of depth layers used to pre-
654 process the acoustic data.

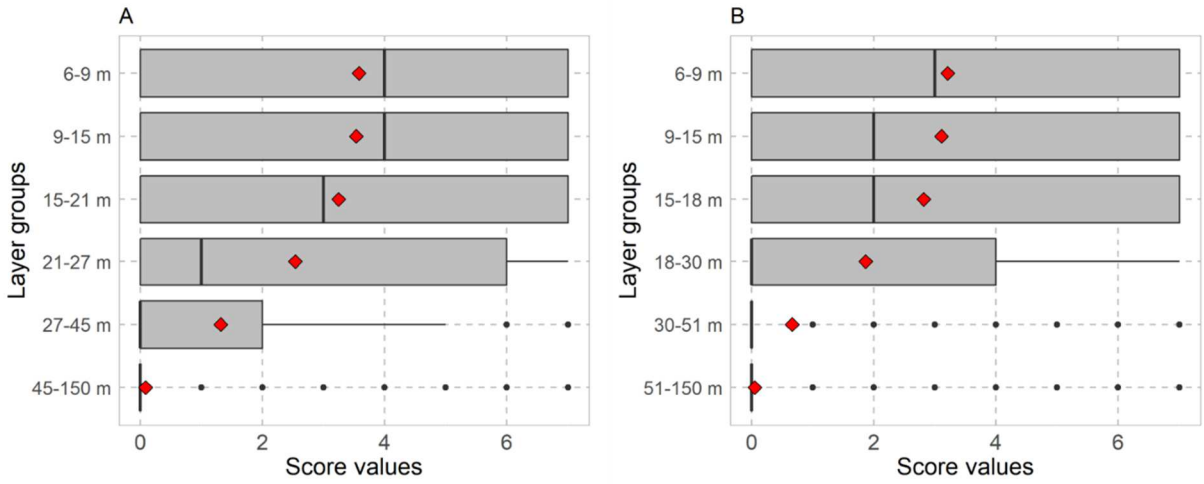

Fig. 4: Boxplot of acoustic score values in the aggregated-layer groups identified by the cluster analysis, for the Atlantic (A), and Indian (B) Oceans. Red diamonds represent mean value of scores in each layer group.

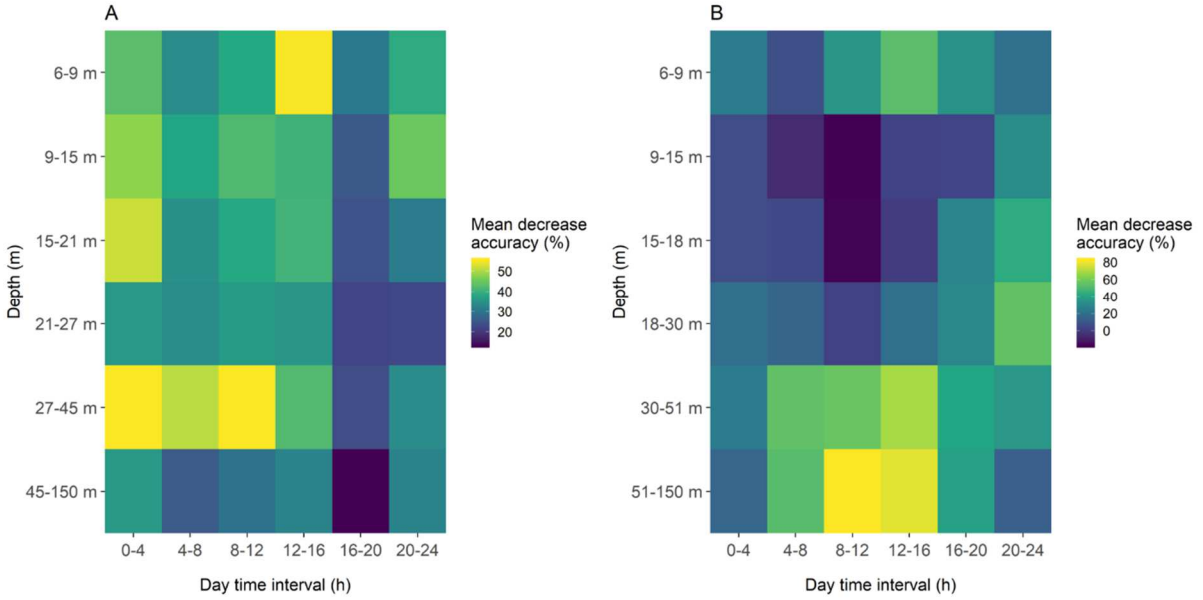

Fig. 5: Importance of depth layers and day period in presence/absence classification for the Atlantic (A) and Indian (B) Oceans. Each cell represents a combination of depth and time period. Colours indicates the importance of the predictor in the classification.

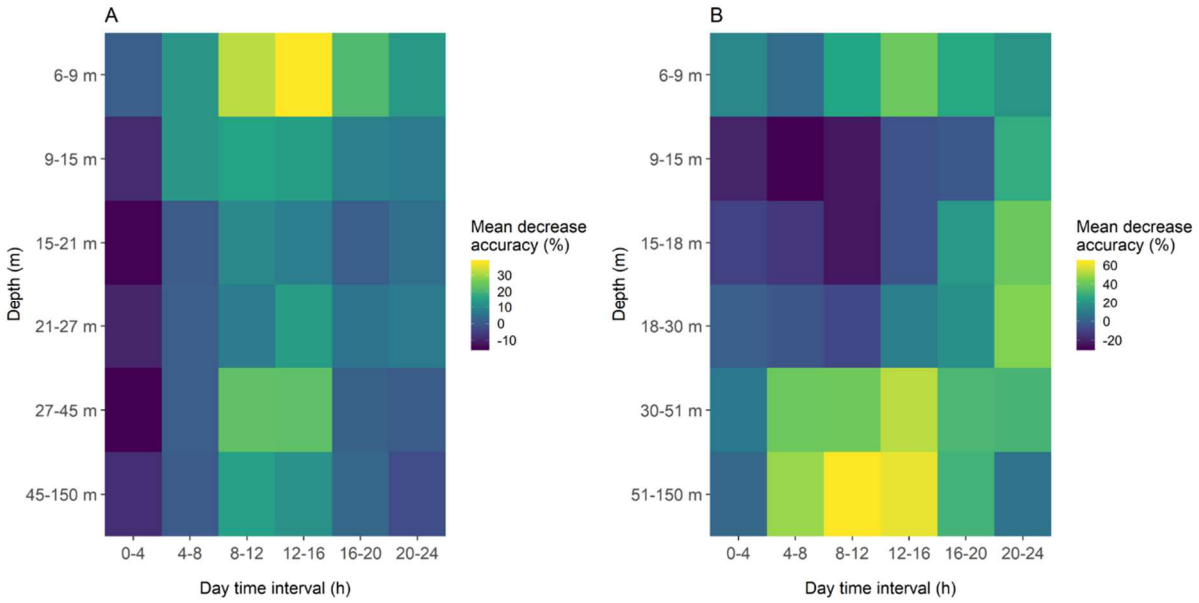

663

664 Fig. 6: Importance of depth layers and day period in multiclass classification for the Atlantic
665 (A) and Indian (B) Oceans. Each cell represents a combination of depth and time period.
666 Colours indicates the importance of the predictor in the classification.